

Vortex matter in superconducting mesoscopic disks: Structure, magnetization, and phase transitions

J. J. Palacios

Department of Physics and Astronomy, University of Kentucky, Lexington, KY 40506, USA
and Departamento de Física Teórica de la Materia Condensada, Universidad Autónoma de Madrid, Cantoblanco, Madrid 28049, Spain.
 (May 17, 2018)

The dense vortex matter structure and associated magnetization are calculated for type-II superconducting mesoscopic disks. The magnetization exhibits generically first-order phase transitions as the number of vortices changes by one and presents two well-defined regimes: A *non-monotonous* evolution of the magnitude of the magnetization jumps signals the presence of a vortex glass structure which is separated by a second-order phase transition at H_{c2} from a condensed state of vortices (giant vortex) where the magnitude of the jumps changes monotonously. We compare our results with Hall magnetometry measurements by Geim et al. (Nature **390**, 259 (1997)) and claim that the magnetization exhibits clear traces of the presence of these vortex glass states.

PACS numbers: 74, 74.60.Ec, 74.76.-w

Electronic device miniaturization in semiconductors has recently reached the ultimate limit where the number of electrons present in the device can be tuned at will even down to a single electron [1,2]. These systems have been given the name of quantum dots or artificial atoms since their generic properties are determined by their few-electron configurations much the same as in real atoms. Analogies can be drawn between these artificial atoms and type-II superconducting mesoscopic disks in perpendicular magnetic fields where the role of the electron is played in this case, not by the Cooper pair, but by another fundamental entity: The vortex. When the dimensions of the disk are comparable to the coherence length ξ only few vortices can coexist in the system. In contrast to the usual triangular arrangement in bulk, complex and unique vortex structures are expected to occur due to the competition between surface superconductivity and vortex-vortex interaction. When the dimensions of the system are much smaller than ξ the very notion of superconductivity needs to be revised [3].

Transport experiments have contributed in a decisive way to unveil the electronic structure of artificial atoms [2]. Similarly, transport measurements [4] in individual mesoscopic disks gave us the first experimental evidence of the structure of the order parameter in these systems. Oscillations of the critical temperature T_c as a function of the external magnetic field H were correctly accounted for by the quantization of the angular momentum L of the Cooper pair wavefunction or, in other words, by transitions between giant vortex states with a different number of flux quanta. Close to the superconductor-normal phase boundary the theoretical analysis of these transitions does not present any difficulty since it simply implies solving the linearized Ginzburg-Landau equations [4-7].

Hall magnetometry [8], on the other hand, is revealing itself as a powerful tool for obtaining information of the order parameter through its associated magnetization M away from the superconductor-normal phase boundary. To date, the theoretical efforts to calculate the structure of the order parameter and M well into the superconducting phase have been mostly restricted to the numerical solving of the Ginzburg-Landau equations under the assumption of an order parameter with a well-defined L [9,10]. This is justifiable for type-I superconducting disks. For type-II disks, however, this assumption is no longer valid. More precisely, it is only expected to hold in the Meissner state, which is associated to an $L = 0$ order parameter, and above H_{c2} where, close to the surface of the disk, the superconductivity can survive up to a higher critical field H_{c3} [4-7]. This surface order parameter is referred to as a giant vortex or macrovortex [9,10]. For $H_{c1} < H < H_{c2}$ it has been argued [9] and shown in numerical simulations of the time-dependent Ginzburg-Landau equations [8,11] that the order parameter can form complex structures of single-fluxoid vortices, i.e., a “budding” Abrikosov lattice. From the more analytic standpoint presented in this paper the appearance of these structures can only come about if the order parameter *does not* have a well-defined L . To find and understand the structure of these vortex states, to calculate the magnetization associated to them, and to link these states to the Abrikosov lattice which emerges in the thermodynamic limit of infinite disks are the main goals of this paper. We do this by expanding the order parameter in an appropriate basis and minimizing, analytically to a large extent, the Ginzburg-Landau functional. For an increasing magnetic field we find first-order phase transitions whenever a vortex is added to the disk. A *non-monotonous* behavior of the magnitude of the mag-

netization jumps signals the presence of the glassy vortex structures while, at H_{c2} , a second-order phase transition constitutes the signature of the condensation of the vortices into the giant vortex state. In addition we compare with the magnetization measured in Al disks by Geim *et al.* in Ref. [8] and claim that the magnetization jumps present a non-monotonous evolution which, as we stated above and shown below, can be associated to the existence of single-fluxoid vortex glassy structures. This would indicate that the Al disks in Ref. [8] behave like type-II superconductors rather than type-I, possibly due to the expected enhancement of the effective magnetic penetration length in such a geometry.

We start from the traditional Ginzburg-Landau functional for the Gibbs free energy of the superconducting state

$$G_s = G_n + \int d\mathbf{r} \left[\alpha |\Psi(\mathbf{r})|^2 + \frac{\beta}{2} |\Psi(\mathbf{r})|^4 + \frac{1}{2m^*} \Psi^*(\mathbf{r}) \left(-i\hbar\nabla - \frac{e^*}{c} \mathbf{A}(\mathbf{r}) \right)^2 \Psi(\mathbf{r}) + \frac{[h(\mathbf{r}) - H]^2}{8\pi} \right], \quad (1)$$

where G_n is the Gibbs free energy of the normal state and $[-i\hbar\nabla - e^*\mathbf{A}(\mathbf{r})/c]^2/2m^*$ is the kinetic energy operator for Cooper pairs of charge $e^* = 2e$ and mass $m^* = 2m$ in a vector potential $\mathbf{A}(\mathbf{r})$ which is associated with the magnetic induction $h(\mathbf{r})$. The parameters α and β have the usual meaning [12]. Before proceeding any further we must stress a not fully appreciated fact: Even for small values of κ (≈ 1), the magnetic induction is weakly varying in space down to fairly low fields ($H \approx 0.5H_{c2}$) [13]. This observation is very important for our purposes since, down to $H \approx 0.5H_{c2}$, it is a very good approximation to consider a uniform magnetic induction [$h(\mathbf{r}) = B$] and to expand of the order parameter in the following way:

$$\Psi(\mathbf{r}) = \sum_{L=0}^{\infty} C_L \frac{1}{\ell\sqrt{2\pi}} e^{-iL\theta} \Phi_L(r). \quad (2)$$

In this expansion $C_L \equiv |C_L|e^{i\phi_L}$ are complex coefficients and $\frac{1}{\ell\sqrt{2\pi}}e^{-iL\theta}\Phi_L(r)$ are normalized nodeless functions that diagonalize, in the symmetric gauge, the kinetic energy operator appearing in Eq. 1 with eigenvalues $\epsilon_L(B)$. We only consider disk thicknesses smaller than the coherence length so that the order parameter can be taken constant in the direction of the field. These eigenfunctions are subject to the boundary conditions of zero current through the surface and the radial part $\Phi_L(r)$ may be found numerically. (The radial unit is the magnetic length $\ell = \sqrt{e^*\hbar/cB}$). This expansion captures both the simplicity of the macrovortex (above H_{c2}) when only one C_L is expected to be different from zero and the full complexity of the order parameter (below H_{c2}) when several L 's must participate.

Direct substitution of the expansion 2 into Eq. 1 and subsequent numerical minimization of the resulting expression is a daunting task bound to fail due to the large

number of unknown variables involved. Instead, it is key to consider expansions in restricted sets $\{L_1, L_2, \dots, L_N\}$ of few N components where $L_1 < L_2 < \dots < L_N$. The Gibbs free energy takes the following form for each set:

$$G_s - G_n = \sum_{i=1}^N \alpha [1 - B\epsilon_{L_i}(B)] |C_{L_i}|^2 + \frac{1}{4} \alpha^2 \kappa^2 B R^2 \times \left[\sum_{i=1}^N I_{L_i}(B) |C_{L_i}|^4 + \sum_{j>i=1}^N 4I_{L_i L_j}(B) |C_{L_i}|^2 |C_{L_j}|^2 + \sum_{k>j>i=1}^N 4\delta_{L_i+L_k, 2L_j} \cos(\phi_{L_i} + \phi_{L_k} - 2\phi_{L_j}) I_{L_i L_j L_k}(B) |C_{L_i}| |C_{L_j}|^2 |C_{L_k}| + \sum_{l>k>j>i=1}^N 8\delta_{L_i+L_l, L_j+L_k} \cos(\phi_{L_i} + \phi_{L_l} - \phi_{L_j} - \phi_{L_k}) I_{L_i L_j L_k L_l}(B) |C_{L_i}| |C_{L_j}| |C_{L_k}| |C_{L_l}| \right] + (B - H)^2, \quad (3)$$

where $G_s - G_n$ and α are given in units of $H_{c2}^2 V/8\pi$ (V is the volume of the disk), $\epsilon_L(B)$ is given in units of the lowest Landau level energy $\hbar\omega_c/2$ (with $\omega_c = e^*B/m^*c$), R is the radius of the disk in units of ξ , and B and H are given in units of H_{c2} . The terms proportional to α contain the condensation and kinetic energy of the Cooper pairs. All the other terms, which are proportional to α^2 , account for the ‘‘interaction’’ between Cooper pairs. There appear four types of these terms: (i) those proportional to $I_L(B) \equiv \int dr r \Phi_L^4$ reflecting the interaction between Cooper pairs occupying the same quantum state L , (ii) those proportional to $I_{L_i L_j}(B) \equiv \int dr r \Phi_{L_i}^2 \Phi_{L_j}^2$ reflecting the interaction between Cooper pairs occupying different quantum states, and (iii) the ones proportional to $I_{L_i L_j L_k}(B) \equiv \int dr r \Phi_{L_i} \Phi_{L_j}^2 \Phi_{L_k}$ and proportional to $I_{L_i L_j L_k L_l}(B) \equiv \int dr r \Phi_{L_i} \Phi_{L_j} \Phi_{L_k} \Phi_{L_l}$ which, along with the phases ϕ_L , are responsible for the correlation between vortices. The non-linear dependence on B of these integrals [as well as that of $\epsilon_L(B)$] comes from the existence of the disk surface.

In order to find the minimum Gibbs free energy for a given set we have to minimize with respect to the moduli $|C_{L_1}|, \dots, |C_{L_N}|$, the phases $\phi_{L_1}, \dots, \phi_{L_N}$ of the coefficients, and with respect to B . The minimum-energy set of components is picked up at the end. The advantage of doing this selective minimization resides in our expectation that a small number of components will suffice to describe the order parameter for the disk sizes considered in the experiment of Ref. [8]. As an illustrative and relevant example we consider in the detail the solution with a single component $\{L\}$. The energy functional is invariant with respect to the phase of the only coefficient so one can minimize analytically with respect to $|C_L|^2$ to obtain

$$G_s - G_n = -\frac{[1 - B\epsilon_L(B)]^2}{\kappa^2 B R^2 I_L(B)} + (B - H)^2. \quad (4)$$

Finally, the minimal value of B and the minimum Gibbs free energy for each L must be found numerically. It is important to notice that α disappears from the final expression in Eq. (4) which leaves us with κ as the only adjustable parameter when comparing with experiments. (This is also true for the more complex cases discussed below). The 2-component $\{L_1, L_2\}$ solutions can be dealt with in a similar way. The energy functional is invariant with respect to the phases so one can minimize analytically with respect to $|C_{L_1}|^2$ and $|C_{L_2}|^2$ and numerically only with respect to B . The final solutions look generically like an $(L_2 - L_1)$ -vortex ring. For 3-component solutions (two vortex rings) the energy functional is still invariant with respect to all the three phases whenever $L_1 + L_3 \neq 2L_2$, and, once again, the minimization with respect to $|C_{L_1}|^2$, $|C_{L_2}|^2$, and $|C_{L_3}|^2$ can be done analytically. However, if $L_1 + L_3 = 2L_2$, the two rings have the same number of vortices and their relative angular positions come into play through the term depending on the phases. There is, however, an obvious choice for these phases: $\phi_{L_1} = 0, \phi_{L_2} = 0, \phi_{L_3} = \pi$. This choice gives a negative contribution to the free energy which reflects the lock-in position between the vortex rings. One important fact should be noted now: The components in which the bulk Abrikosov lattice needs to be expanded in the symmetric gauge are strongly overlapping. Depending on the chosen symmetry of the lattice the set of components is either $\{1, 7, 13, 19, \dots\}$ for the C_6 symmetry with a vortex at the origin or $\{0, 3, 6, 9, \dots\}$ for the C_3 symmetry with the center of a vortex triangle at the origin [14]. Consequently, the minimum-energy solutions for disks are expected to have strongly overlapping components which invalidates any perturbative treatment of the terms that contain the phases [15]. Moreover, unlike simpler geometries [15], there is no direct connection between number of components and number of vortices. This prompts us to seek solutions through numerical minimization with respect to the moduli and B for the 3-component cases just mentioned, and, for $N > 3$, with respect to the moduli, the phases, and B whenever the terms involving phases are present. Fortunately, for the disk sizes like the ones used in the experiment of Ref. [8] we will see below that 2 and 3-component solutions suffice to capture the relevant physics.

Figure 1 shows the magnetization as a function of H for a disk of $R = 8\xi$ and $\kappa = 3$. (There is nothing special about these parameters, the only purpose of which being to be convenient for the discussion of the physics we want to bring up). As indicated in the figure, different types of lines correspond to the magnetization obtained expanding the order parameter with up to $N = 1, 2, 3$, and 4 components. A common feature to all curves is that the magnetization exhibits many first-order transitions. Above H_{c2} the $N = 1$ solutions suffice to describe entirely the order parameter and magnetization. Here the solutions correspond to a giant vortex which con-

tains L (the quantum number of the single component) fluxoids. Whenever L changes by one the magnetization presents a (non-quantized) jump whose magnitude evolves *monotonously* with L . Below H_{c2} we see that the $N = 1$ solutions underestimate the correct value of the magnetization. Allowing more components in the expansion has a fundamental effect: It splits the giant vortex into a complex structure of many single-fluxoid vortices [for an example see Figs. 2(a) to (d)]. This reflects in the magnetization curves by changing the regular evolution of the magnitude of the jumps into an irregular one. Whenever a vortex is added or removed from the disk the symmetry of the new vortex configuration is expected to change which, in turn, expels the field in a different way. There exist configuration switches for a given number of vortices, but these changes *do not* reflect in the magnetization, in contrast to what has been suggested [8]. When the number of vortices is large enough, there are usually two possible symmetries within each magnetization step: One with a vortex at the center of the disk and one without it which are reminiscent of the C_3 and C_6 symmetries of the regular vortex lattice. On top of the many first-order transitions the overall slope in the magnetization clearly changes at H_{c2} , i.e., at the transition between the giant vortex and the vortex glass structures. This transition is reminiscent of the second-order transition at H_{c2} for bulk samples where M vanishes.

Finally, we would like to point out that the magnetization measured by Geim et al. in Ref. [8] presents features that are in good agreement with our results despite of the fact that the disks are made out of a strong type-I material as Al. In these materials the plate geometry can lead to vortex structures being more favorable than domains [16]. To compare with the experiment, we simulate this fact by using a higher value of κ than the nominal one. In Fig. 3 we show the data for a disk of nominal radius $R = 5\xi$, thickness $d = 0.6\xi$, and $\kappa = 0.24$. We have obtained a reasonable good agreement in the number and magnitude of the jumps, and overall shape of the magnetization using $R \approx 5\xi$ and $\kappa \approx 1$ (the dotted line is a good example). This is consistent with an effective penetration length longer than expected and, possibly, with a coherence length shorter than the bulk nominal one. Although, due to the smallness of the disk, it is difficult to point at a second-order phase transition, the non-monotonous evolution of the magnitude of the magnetization jumps is notorious over a large range of fields which, as we have shown, is an indication of the formation of vortex glass structures. In our approximation the magnetic induction is uniform in space, but, given the good agreement with the experimental curve, this seems to be a much less important restriction than considering an order parameter with a well-defined quantum number L [10].

The author acknowledges enlightening discussions with A. K. Geim and thanks him for pointing out to the au-

thor a very recent related work [17]. This work has been funded by NSF Grant DMR-9503814 and MEC of Spain under contract No. PB96-0085.

-
- [1] R. C. Ashoori, *Nature* **379**, 413 (1996).
 - [2] L. Kouwenhoven *et al.*, *Science* **278**, 1788 (1997).
 - [3] F. Braun, Jan von Delft, D. C. Ralph, and M. Tinkham, *Phys. Rev. Lett.* **79**, 921 (1997).
 - [4] V. V. Moshchalkov *et al.*, *Nature* **373**, 319 (1995).
 - [5] R. Benoist and W. Zwerger, *Z. Phys. B* **103**, 377 (1997).
 - [6] A. I. Buzdin, *Phys. Rev. B* **47**, 11 416 (1993).
 - [7] A. Bezryadin, Y. N. Ovchinnikov, and B. Pannetier, *Phys. Rev. B* **53**, 8553 (1996).
 - [8] A. K. Geim *et al.*, *Nature* **390**, 259 (1997).
 - [9] V. V. Moshchalkov, X. G. Qiu, and V. Bruyndoncx, *Phys. Rev. B* **55**, 11 793 (1997).
 - [10] P. S. Deo, V. A. Schweigert, F. M. Peeters, and A. K. Geim, *Phys. Rev. Lett.* **79**, 4653 (1997); V. A. Schweigert and F. M. Peeters, *Phys. Rev. B* **57**, 13 817 (1998).
 - [11] A. López, private communication.
 - [12] M. Tinkham, *Introduction to Superconductivity*, 2nd Ed. (McGraw-Hill, New York, 1996).
 - [13] E. H. Brandt, *Phys. Rev. Lett.* **78**, 2208 (1997).
 - [14] G. M. Braverman, S. A. Gredeskul, and Y. Avishai, *cond-mat/9802287*.
 - [15] J. J. Palacios, *Phys. Rev. B* **57**, 10873 (1998).
 - [16] G. J. Dolan, *J. Low Temp. Phys.* **15**, 111 (1974).
 - [17] V. A. Schweigert, P. S. Deo, F. M. Peeters, *cond-mat/9806013*.

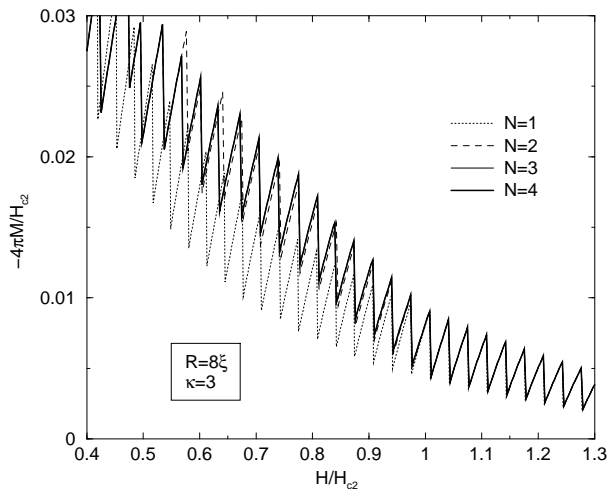


FIG. 1. Magnetization as a function of H for a disk of radius $R = 8\xi$ and $\kappa = 3$. Different line types correspond to different number of components allowed in the minimization. For this specific set of parameters the plot shows clearly the necessity of considering more than one component below H_{c2} . However, no appreciable difference can be seen between the traces obtained using an expansion with up to $N = 3$ and $N = 4$ components.

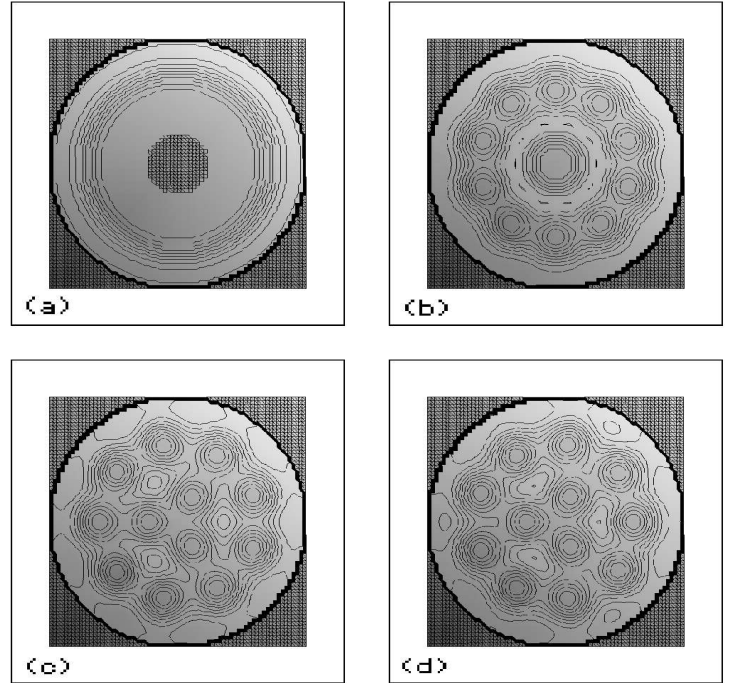


FIG. 2. Modulus square of the order parameter for an $R = 8\xi$, $\kappa = 3$ disk at $H = 0.6H_{c2}$ expanded with up to (a) $N = 1$ (minimum-energy set $\{12\}$), (b) $N = 2$ ($\{3, 12\}$), (c) $N = 3$ ($\{0, 3, 12\}$), and (d) $N = 4$ ($\{0, 3, 6, 12\}$) components. The vortex structure is strongly modified from $N = 1$ to $N = 4$ although the total number of vortices is always given by the largest L which does not depend on the the number of components considered. (Only the internal arrangement of vortices does.) Allowing 4-component solutions does not change appreciably the magnetization obtained with $N = 3$ (or even $N = 2$) at any value of H (see Fig. 1). However, the order parameter is still modified as can be seen by comparing (c) and (d). The addition of a fourth component does not increase the number of vortex rings, but can help fix the relative position of the two existing ones in the $N = 3$ solution. This modification does not have measurable consequences, but illustrates how one of the symmetries of the triangular vortex lattice (the C_3) can emerge, bearing confidence in our calculations.

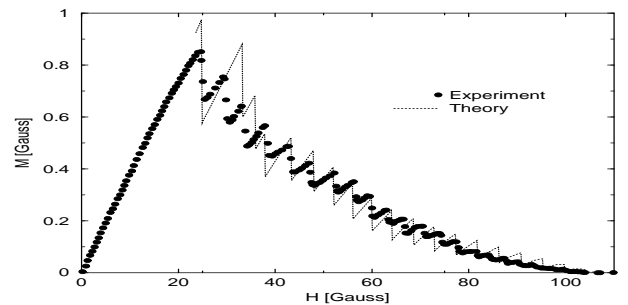


FIG. 3. Comparison between experimental data (reproduced from Refs. [10]) and theory using $R = 5.25\xi$ and $\kappa = 1.2\xi$. Similar considerations as in Refs. [10] have been followed for the adjustment of the theoretical curve.